NON-OBERBECK-BOUSSINESQ NATURAL CONVECTION IN A TALL DIFFERENTIALLY HEATED CAVITY

D. Kızıldağ[*], J. Ventosa[†], I. Rodríguez[†] and A. Oliva[†]

[*] [†]Centre Tecnològic de Transferència de Calor (CTTC),
Universitat Politècnica de Catalunya (UPC),
ETSEIAT, Colom 11, 08222, Terrassa, Barcelona, Spain.
e-mail: cttc@cttc.upc.edu

Key words: Natural Convection, Water, Differentially Heated Cavity, Non-Oberbeck-Boussinesq

Abstract. *Turbulent flow in a water-filled rectangular parallelepiped tank of an integrated solar collector is analyzed by means of a set of two and three dimensional simulations. The geometry and the working conditions of the prototype yield an aspect ratio of $\Gamma = 6.68$, Rayleigh number of $Ra = 2.2 \times 10^{11}$ and a Prandtl number of $Pr = 3.42$. Different coarse DNS simulations and LES simulations using the dynamic Smagorinsky SGS and WALE model are presented. Validity of the Oberbeck-Boussinesq approximation is questioned. Heat transfer and first and second order statistics are studied.*

1 INTRODUCTION

The natural convection flow within enclosures has attracted the attention of many researchers due to its potential to model numerous applications of engineering interest, such as cooling of electronic devices, air flow in buildings, heat transfer in solar collectors, among others. The natural convection studies corresponding to the parallelepipedic enclosures can be classified into two elementary classes: i) heating from a horizontal wall (heating from below); ii) heating from a vertical wall. The characteristic example of the former case is the Rayleigh-Bénard flow, however this work will only focus on the cavities heated from the side. This configuration is referred commonly as the differentially heated cavity.

Although the differentially heated cavity configuration represents a simple geometry, the flow gets complex for sufficiently large Rayleigh numbers [1]. The flow undergoes a gradual transition to a chaotic state as the Rayleigh number reaches a critical value. For the situation studied in this work, both laminar, transitional, and turbulent zones are expected to coexist within the domain. Generally the core of the cavity together with the upstream part of the vertical boundary layers remain laminar while at some point in the downstream part of the vertical boundary layers, turbulent fluctuations become

significant. It is a challenging task to detect this phenomenon [2]. Another important issue is the stratification phenomenon taking place in the core of the cavity. It is one of the basic open problems of this configuration. Comparisons between numerical and experimental studies give quite different results, which may be justified by the thermal radiation effects [3].

The vast majority of the performed work in this field corresponds to air-filled cavities (see [2] for a detailed preview). If the working fluid is water, obtaining solutions for the governing equations gets even more complicated, as the boundary layer becomes thinner than for air at the same conditions. As a consequence, there is an increasing demand for excessively fine grids in space and time for solving the three-dimensional and time dependent flow, in order to capture the smallest scales of the turbulent flow. Direct Numerical Simulations (DNS) can be limited to lower Rayleigh numbers and less time integration, however the use of Large-Eddy Simulations (LES) appears as an atractive alternative for the resolution of natural convection problems at high Rayleigh numbers. It must be borne in mind that as LES performs a modelling for the smallest scales of the flow, the results are strongly dependent not only on grid resolution, but also on the selection of the appropriate subgrid scale stresses (SGS) model to describe the flow behaviour.

Additional to the issues explained above, when investigating the fluid behaviour in real working conditions, the validity of the Oberbeck-Boussinesq approximation has to be questioned. According to Gray and Giorgini [4], the use of the Oberbeck-Boussinesq approximation can be considered valid for variations of thermosphysical properties up to 10% with respect to the mean value.

The main objective of this work is to analyze the turbulent natural convection flow of water in a rectangular parallelepiped tank. This configuration corresponds to an integrated solar collector installed on an advanced façade. The aspect ratio is $\Gamma = 6.68$. The working conditions of the particular design yield a Rayleigh number of $Ra = 2.2 \times 10^{11}$ and a Prandtl number of $Pr = 3.42$. Long-term accurate statistical data by means of a coarse DNS simulation and a LES simulation using the dynamic Smagorinsky SGS model [5] are presented, investigating the characteristics of the turbulent flow within the differentially heated cavity. Detailed results of first and second order turbulent statistics are also presented. Moreover, this work also aims at obtaining a starting point for our study of non-Oberbeck-Boussinesq effects in turbulent natural convection. The actual working conditions of the prototype point out a variation of about 20 % in the dynamic viscosity and 15 % in the thermal expansion coefficient. Thus, it is of interest to analyze some features of turbulent natural convection flow including Oberbeck-Boussinesq effects.

2 DEFINITION OF THE PROBLEM

The adopted geometry considered in this work is shown in Figure 1. This geometry models the parallelepiped tank of an integrated solar collector. The height of the tank (H), and the width (W) are 0.735m and 0.11m respectively, resulting in an aspect ratio of $\Gamma = 6.68$.
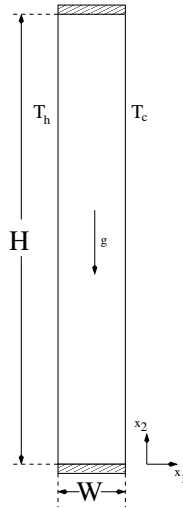
Figure 1: Geometry of the differentially heated cavity

Taking into consideration the real working conditions of the studied prototype, the temperatures at the hot and cold vertical isothermal walls are set to 57 $^\circ C$ and 47 $^\circ C$ respectively.

3 DESCRIPTION OF MATHEMATICAL AND NUMERICAL METHOD

The Navier-Stokes and continuity equations can be written as

$$\mathsf{M}\boldsymbol{u} = \boldsymbol{0} \tag{1}$$

$$\frac{\partial \boldsymbol{u}}{\partial t} + \mathsf{C}\left(\boldsymbol{u}\right)\boldsymbol{u} + \nu\mathsf{D}\boldsymbol{u} + \rho^{-1}\mathsf{G}\boldsymbol{p} + f = \boldsymbol{0} \tag{2}$$

$$\frac{\partial \mathbf{T}}{\partial t} + \mathsf{C}\left(\boldsymbol{u}\right)\mathbf{T} + \rho^{-1}Cp^{-1}k\mathsf{D}(\mathbf{T}) = \boldsymbol{0} \tag{3}$$

where $\boldsymbol{u} \in \mathbb{R}^{3m}$ and $\boldsymbol{p} \in \mathbb{R}^{m}$ are the velocity vector and pressure, respectively (here m applies for the total number of control volumes (CV) of the discretised domain), ν is the kinematic viscosity and ρ the density. f is the body force $f = \beta(T_0 - T_m)g$. Convective and diffusive operators in the momentum equation for the velocity field are given by $\mathsf{C}\left(\boldsymbol{u}\right) = \left(\boldsymbol{u}\cdot\nabla\right) \in \mathbb{R}^{3m\times3m}$, $\mathsf{D} = \nabla^2 \in \mathbb{R}^{3m\times3m}$ respectively. Gradient and divergence (of

a vector) operators are given by $\mathsf{G} = \nabla \in \mathbb{R}^{3m \times 3m}$ and $\mathsf{M} = \nabla \cdot \in \mathbb{R}^{m \times 3m}$ respectively.

In bouyancy driven flows a common approach is to consider constant thermophysical properties of the fluid, with the exception of the density variations that are only taken into account in the bouyancy forces, i.e., the so-called Oberbeck-Boussinesq approximation. Thus, the temperature dependency of density is linearized in the bouyancy force as:

$$\rho(T) = \rho_m - \rho_m \beta_m (\mathbf{T} - T_m) \tag{4}$$

Here $T_m = (T_h - T_c)/2$ is the mean value of the temperatures of the cold and hot walls. Those assumptions have its own implications. First, continuity equation is treated in its incompressible form, neglecting acoustic phenomena, which in the case of liquids has no major implications. However, for liquids, deviations from the aforementioned hypothesis are mainly due to viscosity variations, as the viscosity strongly decreases with the temperature increase.

When considering these effects (Non-Oberbeck-Boussinesq effects) in our work, the following are assumed:

- temperature dependent thermophysical properties

- density variations are only taken into account in the bouyancy term

- the temperature dependence of the density is linearized as:

$$\rho(T) = \rho_m - \rho'(T) \tag{5}$$

Under the above assumptions, equations 1-3 read:

$$\mathsf{M}\boldsymbol{u} = \mathbf{0} \tag{6}$$

$$\frac{\partial \boldsymbol{u}}{\partial t} + \mathsf{C}\left(\boldsymbol{u}\right)\boldsymbol{u} + \mathsf{D}(\nu(T)\boldsymbol{u}) + \rho_m^{-1}\widehat{\mathsf{G}}\boldsymbol{p} - \rho_m^{-1}\rho'(T)\mathbf{g} = \mathbf{0} \tag{7}$$

$$\frac{\partial \mathbf{T}}{\partial t} + \mathsf{C}\left(\boldsymbol{u}\right)\mathbf{T} + \rho_m^{-1}Cp_m^{-1}\mathsf{D}(k(T)\mathbf{T}) = \mathbf{0} \tag{8}$$

The temperature dependencies for $\nu(T)$, $k(T)$ and $\rho(T)$ are taken from Furukawa.[6]

Considering the reference scales for length, time, velocity, temperature and dynamic pressure as H, $(H^2/\alpha)Ra^{-0.5}$, $(\alpha/H)Ra^{0.5}$, $T_h - T_c$, $\rho(\alpha/H^2)Ra$, respectively, Non-Oberbeck-Boussinesq thermal convection in the cavity is governed by the non-dimensional quantities: $Ra = (g\beta_m \Delta T_{ref} H^3 Pr_m)/\nu_m^2$, $Pr_m = \nu_m/\alpha_m$, Γ and the non-dimensional thermophysical properties: $\nu* = \nu(T)/\nu_m$; $k^* = k(T)/k_m$; $\rho^* = \frac{\rho_m - \rho(T)}{\rho_m \beta_m \Delta T_{ref}} = \frac{\rho'(T)}{\rho_m \beta_m \Delta T_{ref}}$.

The governing equations are discretized on a collocated unstructured grid arrangement, by means of second-order spectro-consistent schemes [7]. Such discretization preserves the symmetry properties of the continuous differential operators, i.e., the conservation properties are held if, the convective term is discretized by a skew-symmetric operator and the diffusive term is approximated by a symmetric, positive-definite coefficient matrix. These properties ensure both, stability and conservation of the global kinetic-energy balance on any grid. Energy transport is also discretized by means of a spectro-consistent scheme. An explicit third-order Gear-like scheme [8] based on a fractional step method is used for time-advancement algorithm, except for the pressure gradient where a first-order backward Euler scheme is used.

Collocated meshes do not conserve kinetic energy when fractional step method is used [9, 10]. The source of these errors are interpolation schemes and inconsistency in the pressure field, in order to ensure mass conservation. While the first is eliminated through the use of consevative schemes, the latter equals to $\epsilon_{ke} = (\tilde{\boldsymbol{p}}_c)^* \mathsf{M}_c (\mathsf{G}_c - \mathsf{G}_s) \tilde{\boldsymbol{p}}_c$. Felten and Lund [10] showed that pressure errors are of the order of $\mathcal{O}(\triangle x^2 \triangle t)$. However, these errors do not have significant impact on the grid resolutions and time-steps used in LES and DNS.

LES studies have been performed using two different SGS models: i) the dynamic eddy viscosity model (DEV)[5] ii) the wall-adapting local-eddy viscosity (WALE)[11]. In order to study the influence of the models, a course DNS (CDNS) is also calculated.

3.1 Boundary conditions and fluid properties

For the velocities, no-slip condition is applied on all the walls. In the spanwise direction (when applicable) periodic boundary condition is used.

Isothermal vertical walls are assumed. Left vertical wall is at $57~^\circ C$ and right vertical wall is at $47~^\circ C$. In the top and bottom confining walls, Neumann boundary condition ($\partial T / \partial n = 0$) is applied.

Except for the Non-Oberbeck-Boussinesq calculations, the fluid properties for water are calculated at the average temperature of $(T_h - T_c)/2 = 52^\circ C$. Rayleigh number based on the height of the cavity is $Ra = \rho \beta (T_h - T_c) H^3 / \nu \alpha = 2.2 \times 10^{11}$ and the Prandtl number is $Pr = \nu / \alpha = 3.42$, being ν is the kinematic viscosity and α thermal diffusivity.

3.2 Geometric discretization

The samallest scales at the hot and cold walls are imposed by viscous and thermal boundary layers, while grid size at the bulk must be lesser than Kolmogorov scale. For the Prandtl number in our problem, the thermal boundary layer is thinner than the viscous boundary layer as $\delta_t \sim h/Ra^{0.25}$ and $\delta_v \sim Pr^{0.5}\delta_t$ [12]. The meshes shown in Table 1 are used for our preliminary studies.

level	N_1	$\Delta x_{1\,min}$	N_2	$\Delta x_{2\,min}$	Δt
m1	80	4.08×10^{-5}	250	4×10^{-3}	9.12×10^{-6}
m2	176	8.16×10^{-5}	550	1.82×10^{-3}	3.65×10^{-5}
m3	258	6.80×10^{-5}	770	1.30×10^{-3}	2.53×10^{-5}

Table 1: Space and time discretization grids used in the test cases.

4 PRELIMINARY RESULTS AND CONCLUSIONS

As the numerical effort to carry out the present simulations is too large, all the calculations here presented are restricted to two-dimensional (2D) simulations. Although 2D calculations might affect the fluid dynamics, some of the characteristics of the flow or non-Oberbeck-Boussinesq effects can still be captured under this assumption. It has been shown earlier by Trias et al. [2] for a differentially heated cavity for Rayleigh numbers up to 10^{10} and by Schalzl et al. [13] for Rayleigh-Benard convection, that in general as a rough approach to capture the general features of the flow and especially boundary layer profiles and Nusselt numbers, 2D simulations can be a good approximation. This is particulary true for comparisons of the non-Oberbeck-Boussinesq effects, where no SGS model has been used. However, regarding to LES modelling, some of the conclusions drawn in the present work must be taken as preliminary results, as the filtering process might be affected by the 2D assumptions done.

4.1 Grid study

Numerical solutions using grid sizes m_2 and m_3 are compared. Although not shown here, differences are insignificant in terms of heat transfer. However, the differences in velocity profiles are considerable and second order turbulent statistics differ significantly (see Figures 2 and 3).

The integration period for the presented results is 100 time units starting from $t_{ini} = 250$. Even though, more time integration can be necessary, the obtained results suggest using denser grids. Note that coarse mech solution overestimates the peak values of the Reynolds stresses by more than twice.
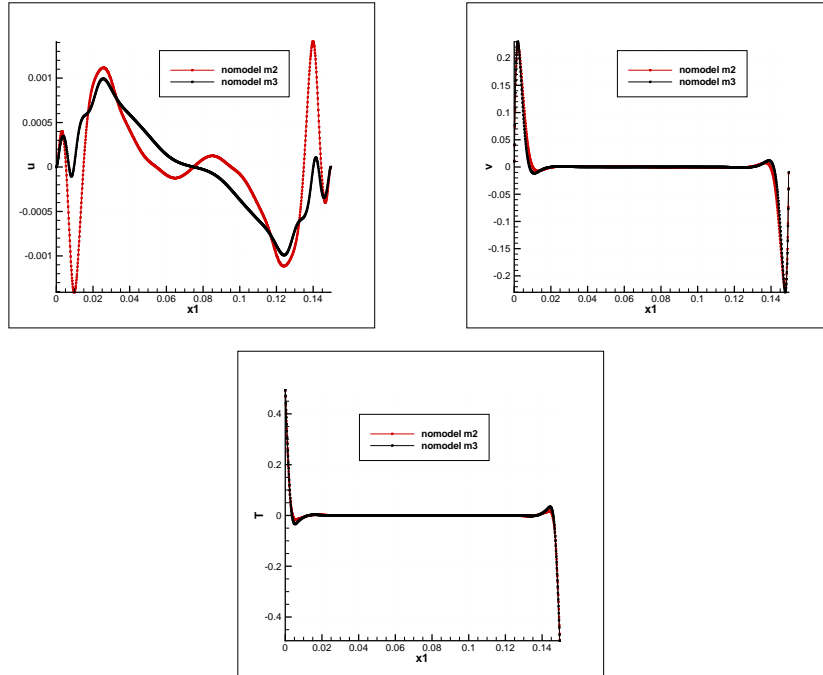
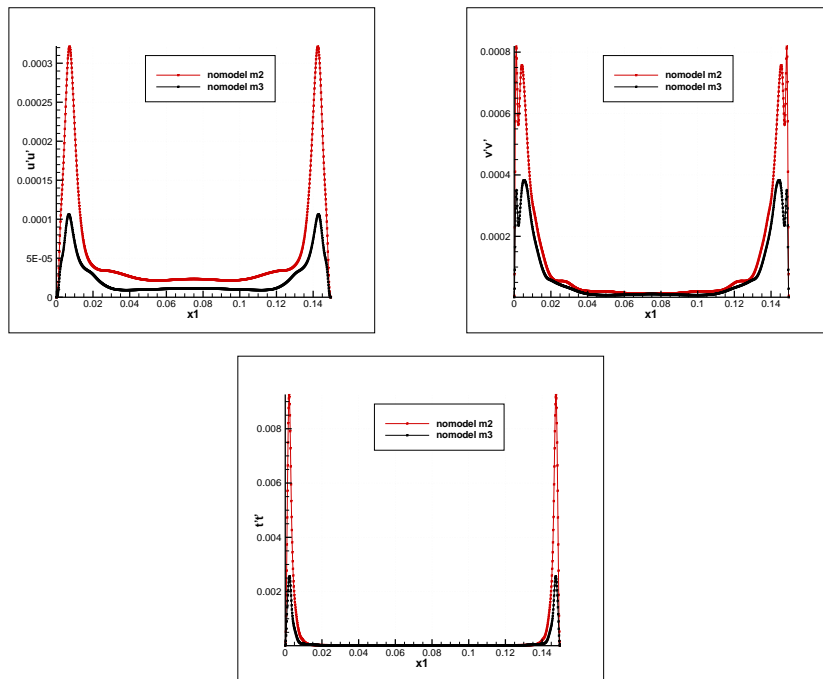Figure 2: Velocity and temperature profiles at $x_2 = 0.5$

Figure 3: Reynolds stress components and temperature variance profiles at $x_2 = 0.5$.

4.2 LES models

In this work, LES studies using two different SGS models (WALE and DEV) have been carried out. The performed numerical solutions with LES models use m_2 grid level.
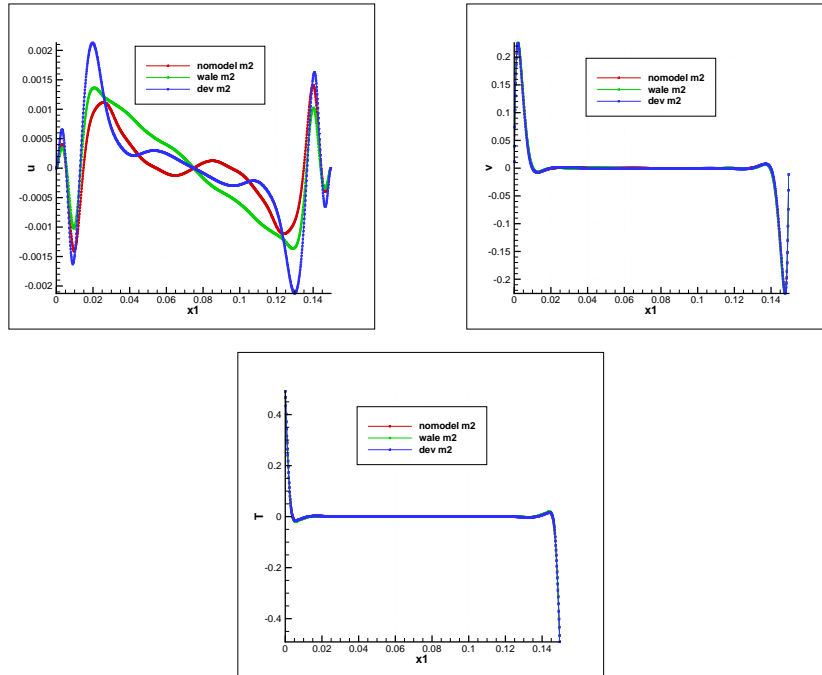

Figure 4: Velocity and temperature profiles at $x_2 = 0.5$

As it can be seen from Figures 4 and 5, for the used mesh size, a clear effect of the LES models cannot be observed. This can be due to the fact that the filtering process employed can be affected by the 2D flow assumption.

In Figure 6 stratification values for the different LES and nomodel cases are shown. Considering the outcome of these preliminary results, one can state that LES models might need relatively more integration time to reach time-independent solution.

These results, together with the outcome of the nomodel comparisons, suggest the employement of the LES models on grid size m_3.
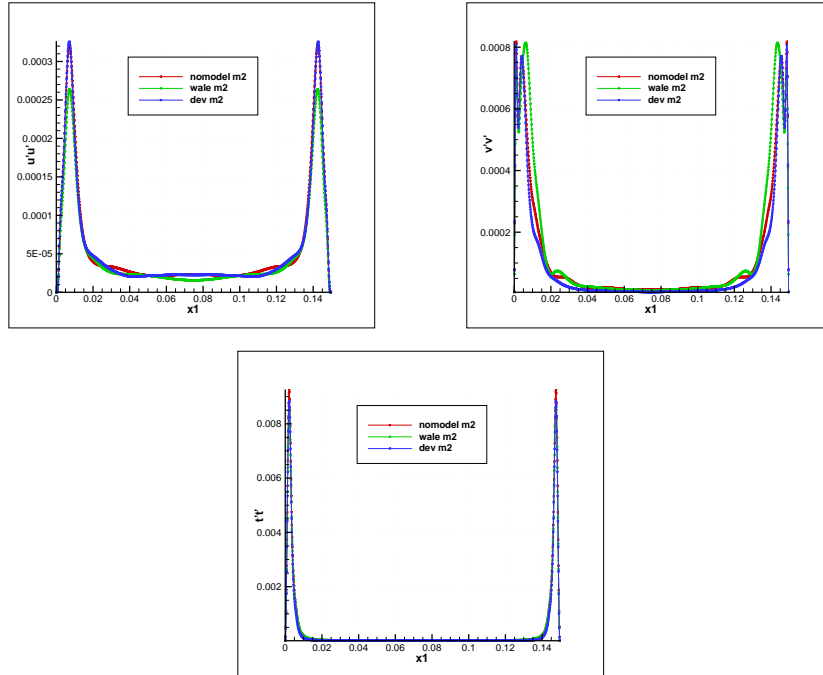
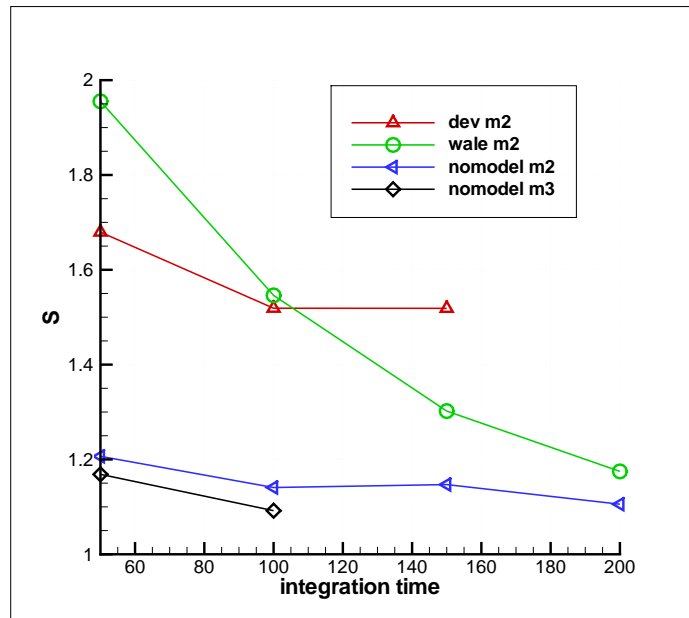Figure 5: Reynolds stress components and temperature variance profiles at $x_2 = 0.5$.

Figure 6: Stratification values for LES models and nomodel cases

4.3 Non-Oberbeck-Boussinesq solutions

In order to study the Non-Oberbeck-Boussinesq effects, m_2 grid size ise used. The presented results correspond to a time integration of 100 time units starting from $t_{ini} = 250$.

First results show clearly that the employement of Oberbeck-Boussinesq approximation affects the thermal and fluid dynamic behaviour of the numerical solution. The influence of considering variable thermophysical properties can be apreciated in Figure 7. On the left, temperature profiles over $x_2 = 0.5$ is plotted. Temperature at the core of the cavity is significantly greater in Non-Oberbeck-Boussinesq solution ($T_{cNOB} > T_{cOB}$). On the right, vertical velocity profile is shown. It can be observed that there is no symmetry in Non-Oberbeck-Boussinesq solution. Boundary layer thickness differs in hot and cold vertical walls. In Figures 8 and 9 isotherms at representative instants for both cases are presented. In these figures, the aforementioned differences can be observed.
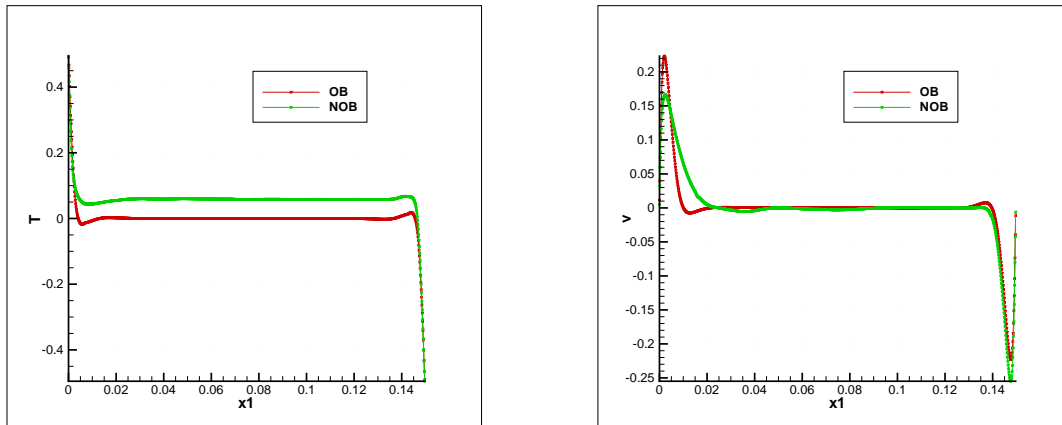

Figure 7: Temperature (left) and vertical velocity (right) profiles at $x_2 = 0.5$

Although some three dimensional simulations have been carried out, the results are not shown here. The present work is intended to be a starting point for our study of non-Oberbeck-Boussinesq effects in turbulent natural convection.
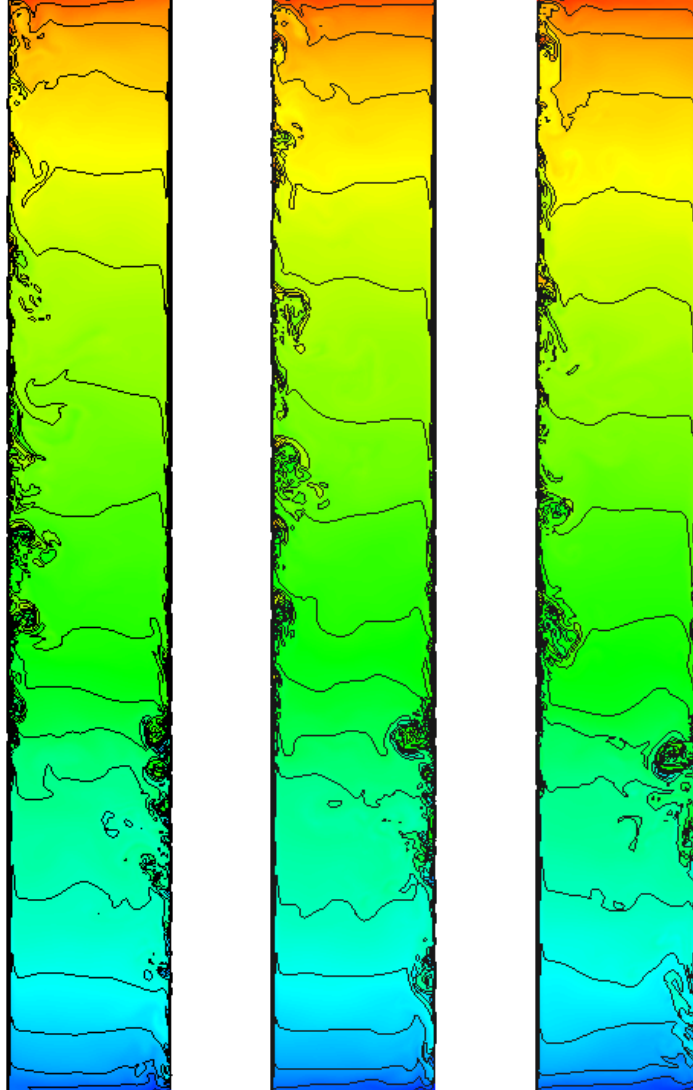
Figure 8: Representative instantaneous isotherms for non-Oberbeck-Boussinesq solution using m_2 mesh. (left) $t = 300$, (middle) $t = 350$, (right) $t = 400$. The isotherms are uniformly dsitributed from -0.5 to 0.5
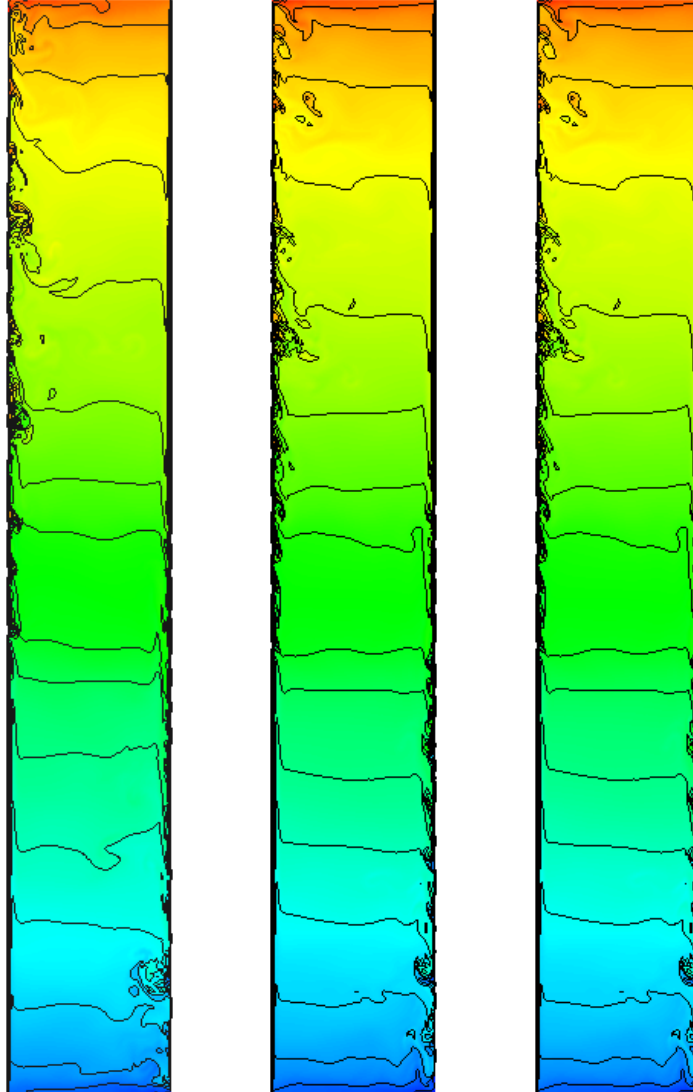
ACKNOWLEDGEMENTS

Figure 9: Representative instantaneous isotherms for Oberbeck-Boussinesq solution using m_2 mesh. (left) $t = 300$, (middle) $t = 350$, (right) $t = 400$. The isotherms are uniformly dsitributed from -0.5 to 0.5

REFERENCES

[1] D.G. Barhaghi and L. Davidson. Natural convection boundary layer in a 5:1 cavity. *Physics of Fluids*, 19(125106), 2007.

[2] X. Trias, M. Soria, D. Perez-Segarra, and A. Oliva. Direct Numerical simulations of two and three dimensional turbulent natural convection flows in a differentialy heated cavity of aspect ratio 4. *Journal of Fluid Mechanics*, 586:259–293, 2007.

[3] S. Xin, J. Salat, P. Joubert, A. Sergent, and P. Le Quere. Three dimensional numer-

ical simulations of turbulent natural convection in an air-filled differentially heated cavity. In *13th International Heat Transfer Conference*, 2006.

[4] D.D. Gray and A. Giorgini. The Validity of Boussinesq Approximation for Liquids and Gases. *Int. J. Heat Mass Transfer*, 19:545–551, 1976.

[5] M. Germano, U. Piomelli, P. Moin, and W.H. Cabot. A dynamic subgrid-scale eddy viscosity model. *Physics of Fluids A*, 3(1760), 1991.

[6] M. Furukawa. Practical expressions for thermodynamic and transport properties of commonly used fluids. *Journal of Thermophysics*, 5(4):524–531, 1991.

[7] R. W. C. P. Verstappen and A. E. P. Veldman. Symmetry-Preserving Discretization of Turbulent Flow. *Journal of Computational Physics*, 187:343–368, May 2003.

[8] G.M. Fishpool and M.A. Leschziner. Stability bounds for explicit fractional-step schemes for the Navier-Stokes equations at high Reynolds number. *Computers and Fluids*, 38:1289–1298, 2009.

[9] Y. Morinishi, T.S. Lund, O.V. Vasilyev, and P. Moin. Fully conservative higher order finite difference schemes for incompressible flow. *Journal of Computational Physics*, 143(1):90–124, 1998.

[10] F.N. Felten and T.S. Lund. Kinetic energy conservation issues associated with the collocated mesh scheme for incompressible flow. *Journal of Computational Physics*, 215(2):465–484, 2006.

[11] F. Nicoud and F. Fucros. Subgrid-scale stress modelling based on the square of the velocity gradient tensor. *Flow, Turbulence and Combustion*, 62:183–200, 1999.

[12] J. Patterson and J. Imberger. Unsteady natural convection in a rectangular cavity. *J. Fluids Mech.*, 100:65–86, 1980.

[13] J. Schmalzl, M. Breuer, and U. Hansen. On the validity of two-dimensional numerical approaches to time-dependent thermal convection. *Europhys. Lett.*, 67 (3):390–396, 2004.